J|A|C|S ARTICLES

Published on Web 08/05/2009

Origins of the Distortions in the Base Pair Step Adjacent to Platinum Anticancer Drug−DNA Adducts. Fundamental NMR Solution Studies Utilizing Right-Handed Cross-Link Models Having 5′- and 3′-Flanking Residues

Jamil S. Saad,[†,‡] Giovanni Natile,[§] and Luigi G. Marzilli*[,†]

Departments of Chemistry, Louisiana State University, Baton Rouge, Louisiana 70803, and Emory University, Atlanta, Georgia 30322, and Dipartimento Farmaco-Chimico, Università di Bari, Via E. Orabona 4, 70125 Bari, Italy

Received May 10, 2009; E-mail: lmarzil@lsu.edu

Abstract: For DNA duplexes, the Lippard laboratory has shown that the XG* base pair (bp) step has a very unusual slide and shift, where G* is a G platinated at N7 by di- or monofunctional platinum anticancer drugs. One approach toward understanding the cause of this important unexpected XG* distortion is to examine single-strand (ss) oligonucleotide (oligo) models. Both duplex and ss XG*G* models of the key G*G* cross-link formed by cisplatin have the HH1 conformation with head-to-head bases. Cross-links have R canting (3′-G* H8 atom toward 5′-G*) in duplexes and L canting (5′-G* H8 atom toward 3′-G*) in ss models. However, dynamic motion in solution makes the ss features difficult to define. Thus, we employ less dynamic cross-link models such as (*R*,*S*,*S*,*R*)-BipPt(d(TG*G*)) and (*R*,*S*,*S*,*R*)-BipPt(d(pG*G*TTT)), the first examples of an HH1 conformer with R canting for ss oligos longer than d(GpG) (Bip = 2,2′-bipiperidine). In these, the 5′-T residue decreases R canting (indicating steric clashes with the 5′-G*) and the less bulky 5′-phosphate group forms a H-bond to HN−Pt (indicating that R canting allows H-bonding). We conclude that the 5′-X residue in duplex adducts changes its position from that in B form DNA to avoid steric clashes with the 5′-G* and the carrier ligand and secondarily to form a Watson−Crick base pair. These features, possibly aided by weak carrier-ligand H-bonding, lead to the relatively unusual features distinctive to the "Lippard bp step".

Introduction

Cisplatin (*cis*-$Pt(NH_3)_2Cl_2$) and its close analogues are the most widely used anticancer agents.[1−6] Addition of cisplatin to DNA forms several classes of DNA adducts; in the most frequent adduct, Pt attacks adjacent G residues, binding at N7 to form an intrastrand cross-link lesion (Figure 1).[6−11] This *cis*-$Pt(NH_3)_2$(d(G*G*)) intrastrand lesion, which is thought to promote cell death, adopts primarily a head-to-head (HH) arrangement, with both G* residues maintaining the *anti* conformation typically found in B-DNA (the asterisk designates a N7-platination).[10,12,13] We call this conformation HH1, Figures 1 and 2. In contrast, the G* bases in the minor G*−Pt−G* interstrand lesion adopt a head-to-tail (HT) conformation.[14−18]

Examination of an X-ray structure of an HMG-bound 16-oligomer[19] and an X-ray/NMR-derived model of a duplex 9-oligomer,[20] both containing the intrastrand cisplatin lesion, led us to focus on the base pair (bp) step between the 5′-flanking bp (X•X′) and the bp with the 5′-G* (G*•C) in duplexes with

[†] Louisiana State University and Emory University.
[‡] Current address: Department of Microbiology, University of Alabama at Birmingham, 845 19th St. S., Birmingham, AL 35294.
[§] Università di Bari.

(1) Wang, D.; Lippard, S. J. *Nat. Rev. Drug Discovery* **2005**, *4*, 307–320.
(2) Centerwall, C. R.; Goodisman, J.; Kerwood, D. J.; Dabrowiak, J. C. *J. Am. Chem. Soc.* **2005**, *127*, 12768–12769.
(3) Decatris, M. P.; Sundar, S.; O'Byrne, K. J. *Cancer Treat. Rev.* **2004**, *30*, 53–81.
(4) Hambley, T. W. *J. Chem. Soc., Dalton Trans.* **2001**, 2711–2718.
(5) Jamieson, E. R.; Lippard, S. J. *Chem. Rev.* **1999**, *99*, 2467–2498.
(6) Lippert, B. *Cisplatin. Chemistry and Biochemistry of a Leading Anticancer Drug*; Wiley-VCH: Weinheim, Germany, 1999.
(7) Ober, M.; Lippard, S. J. *J. Am. Chem. Soc.* **2008**, *130*, 2851–2861.
(8) Ohndorf, U.-M.; Lippard, S. J. In *DNA Damage Recognition*; Siede, W., Kow, Y. W., Doetsch, P. W., Eds.; CRC: Boca Raton, FL, 2005; Vol. 12, pp 239−261.
(9) Chaney, S. G.; Campbell, S. L.; Temple, B.; Bassett, E.; Wu, Y.; Faldu, M. *J. Inorg. Biochem.* **2004**, *98*, 1551–1559.
(10) Bloemink, M. J.; Reedijk, J. In *Metal Ions in Biological Systems*; Sigel, A., Sigel, H., Eds.; Marcel Dekker, Inc.: New York, 1996; Vol. 32, pp 641−685.
(11) Reedijk, J. *Chem. Commun.* **1996**, 801–806.
(12) Sherman, S. E.; Gibson, D.; Wang, A.; Lippard, S. J. *J. Am. Chem. Soc.* **1988**, *110*, 7368–7381.
(13) Sherman, S. E.; Lippard, S. J. *Chem. Rev.* **1987**, *87*, 1153–1181.
(14) Ano, S. O.; Kuklenyik, Z.; Marzilli, L. G. In *Cisplatin. Chemistry and Biochemistry of a Leading Anticancer Drug*; Lippert, B., Ed.; Wiley-VCH: Basel, Switzerland, 1999; pp 247−291.
(15) Coste, F.; Malinge, J.-M.; Serre, L.; Shepard, W.; Roth, M.; Leng, M.; Zelwer, C. *Nucleic Acids Res.* **1999**, *27*, 1837–1846.
(16) Huang, H.; Zhu, L.; Drobny, G. P.; Hopkins, P. B.; Reid, B. R. *Science* **1995**, *270*, 1842–1845.
(17) Paquet, F.; Perez, C.; Leng, M.; Lancelot, G.; Malinge, J.-M. *J. Biomol. Struct. Dyn.* **1996**, *14*, 67–77.
(18) Pinto, A. L.; Lippard, S. J. *Biochim. Biophys. Acta* **1985**, *780*, 167–180.
(19) Ohndorf, U.-M.; Rould, M. A.; He, Q.; Pabo, C. O.; Lippard, S. J. *Nature* **1999**, *399*, 708–712.
(20) Marzilli, L. G.; Saad, J. S.; Kuklenyik, Z.; Keating, K. A.; Xu, Y. *J. Am. Chem. Soc.* **2001**, *123*, 2764–2770.

 10.1021/ja903787m CCC: $40.75

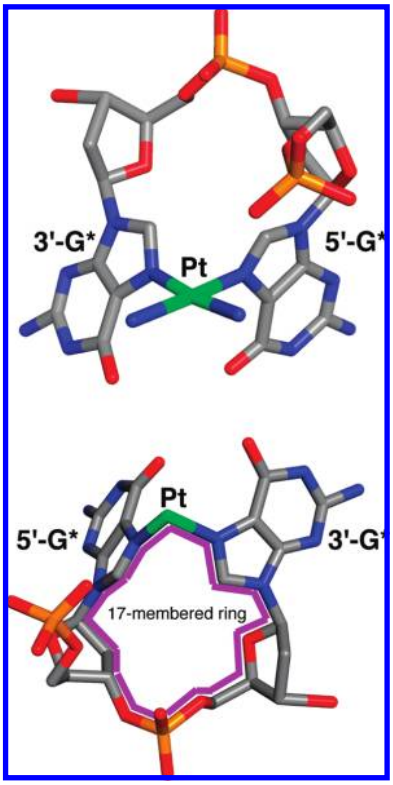

Figure 1. A representative structure of the Pt(G*pG*) cross-link. Top: Pt links adjacent G* residues to form the typical HH1 conformer. Bottom: A different view of the same molecule rotated to show the 17-membered chelate ring in an HH1 G*G* lesion and the *anti* conformation of the G* residues. The 17-membered ring is outlined in purple. These figures were generated by using molecule R1, one of the four *cis*-Pt$(NH_3)_2$(d(pG*pG*)) structures characterized by X-ray crystallography.[12]

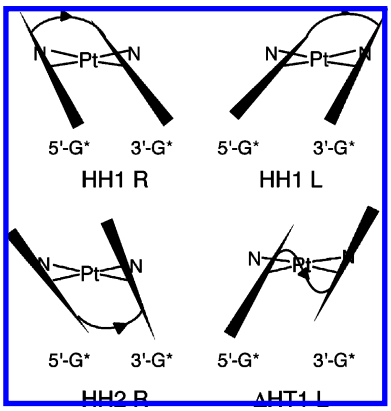

Figure 2. Schematic representation of right (R) and left (L) base canting for the Pt(d(G*pG*)) macrocyclic chelate ring of previously observed HH1, HH2, and ΔHT1 conformers. G* bases are shown as triangles, with the apex of the triangle representing the five-membered ring and the base of the triangle representing the six-membered ring.

the *cis*-Pt$(NH_3)_2$(d(G*G*)) intrastrand cross-link. This XG* bp step is unusual; it has a large positive slide and shift both in solution and in the HMG-bound adduct in the solid state.[19,20] We refer to this unusual bp step as the Lippard bp step because the features were first discovered by crystallographic methods in the Lippard laboratory.[19] At the time of this important finding, it was not realized that the bp step existed in other situations. Our solution studies establish that this distorted step also exists in solution for many duplexes with an intrastrand lesion of the types d(XG*G*) and d(XA*G*) (X = T or C).[20] The d(A*G*) cross-link is the second most abundant lesion.[10] Instead of the normal S pucker, the sugars in the XG* residues have an N pucker.[14,19,20] The X·X′ bp has essentially normal Watson−Crick (WC) H-bonding, but the 5′-G*·C bp is highly dynamic. These features of the Lippard bp step were essential in understanding previously difficult-to-interpret NMR data.[20] This step has grown in significance with the finding that a closely related bp step with a large positive slide and shift exists in the solid state when G* is an adduct of a monofunctional, very promising Pt anticancer drug.[21,22]

Interpretation of factors leading to distortions and structural features in duplexes relies in part on comparison with these features in simpler models, such as single-strand (ss) oligonucleotides (oligos) and even mononucleotides. The G*G* cross-link in duplexes with the Lippard bp step exists as the HH1 conformer, which has head-to-head bases, *anti* G* residues, and a sugar phosphate backbone propagating in the normal direction (Figure 2). In addition, we designate the cross-link in duplexes as HH1 R because it has right-handed canting.[14,20,23,24] Clockwise rotation of the bases (∼45°) leads to left-handed (L) canting, Figure 2. In ss models, canting is usually L;[25,26] one NH in the amine *cis* to the canted 5′-G* base always has a H-bond to the oligo in solid-state structures,[12,27] and the X residue has an S-sugar.[27−30] L canting is associated with strong H-bonding and is found almost universally in single-strand adducts. For duplex models, evidence from both solution and X-ray structures[19,20] suggests that one of the cisplatin NH_3 groups has a long and perhaps weak H bond to the phosphodiester group 5′ to the 5′-G* (designated as XpG*).

A clear understanding of the features of ss models and the differences between the ss and duplex models could help to identify the underlying causes of the distortion in the d(XG*G*) region of DNA. The reasons for the differences between ss and duplex models, such as L vs R canting, are poorly understood. The difference in canting has been recognized for a long time.[26] However, possible differences in sugar pucker and amine H-bonding are not so well established, with investigations on duplexes often having reached different conclusions with regard to pucker and H-bonding.[14,20] Although the controversy about properties has focused on the duplexes, properties of ss adducts may not be as clear as one might suspect from their simplicity.[12,25−29,31−33] This uncertainty arises because *cis*-Pt$(NH_3)_2$(d(G*pG*)) and ss *cis*-Pt$(NH_3)_2$(oligo) models suffer

(21) Lovejoy, K. S.; Todd, R. C.; Zhang, S.; McCormick, M. S.; D'Aquino, J. A.; Reardon, J. T.; Sancar, A.; Giacomini, K. M.; Lippard, S. J. *Proc. Natl. Acad. Sci. U.S.A.* **2008**, *105*, 8902–8907.
(22) Todd, R. C.; Lippard, S. J. In *Platinum and Other Heavy Metal Compounds in Cancer Chemotherapy*; Bonetti, A., Leone, R., Muggia, F. M., Howell, S. B., Eds.; Humana Press: Totowa, NJ, 2009; pp 67−72.
(23) Kline, T. P.; Marzilli, L. G.; Live, D.; Zon, G. *J. Am. Chem. Soc.* **1989**, *111*, 7057–7068.
(24) Yang, D.; van Boom, S.; Reedijk, J.; van Boom, J.; Wang, A. *Biochemistry* **1995**, *34*, 12912–12920.
(25) Girault, J.-P.; Chottard, G.; Lallemand, J.-Y.; Chottard, J.-C. *Biochemistry* **1982**, *21*, 1352–1356.
(26) Kozelka, J.; Fouchet, M. H.; Chottard, J.-C. *Eur. J. Biochem.* **1992**, *205*, 895–906.
(27) Admiraal, G.; van der Veer, J. L.; de Graaff, R. A. G.; den Hartog, J. H. J.; Reedijk, J. *J. Am. Chem. Soc.* **1987**, *109*, 592–594.
(28) den Hartog, J. H. J.; Altona, C.; van der Marel, G. A.; Reedijk, J. *Eur. J. Biochem.* **1985**, *147*, 371–379.
(29) Fouts, C. S.; Marzilli, L. G.; Byrd, R.; Summers, M. F.; Zon, G.; Shinozuka, K. *Inorg. Chem.* **1988**, *27*, 366–376.
(30) Neumann, J.-M.; Tran-Dinh, S.; Girault, J.-P.; Chottard, J.-C.; Huynh-Dinh, T.; Igolen, J. *Eur. J. Biochem.* **1984**, *141*, 465–472.
(31) Berners-Price, S. J.; Ranford, J. D.; Sadler, P. J. *Inorg. Chem.* **1994**, *33*, 5842–5846.

from another deficiency, namely, the "dynamic motion problem".[14,34−37] Central to this deficiency is the inadequacy of ^{1}H NMR methods to allow one to distinguish between a single conformer or a mixture of rapidly interconverting conformers for these models. The simplest models with unlinked guanine derivatives such as *cis*-Pt(NH$_3$)$_2$(GMP)$_2$ have been thought to exist as a mixture of conformers rapidly interconverting via Pt−N7 bond rotation,[38] while essentially only one conformer, HH1, has been implicit in the analyses of the ss adducts.[10,12,13,24−26,32,39] Underlying this interpretation is the assumption that, relative to the NMR time scale, Pt−G* N7 bond rotation is slow in linked intrastrand models.[31] The relatively large G* bases form part of a 17-membered macrocyclic ring in the *cis*-Pt(NH$_3$)$_2$(d(G*pG*)) adduct and would appear to be unable to rotate freely (Figure 1). However, there is no strong evidence to support this assumption. Indeed, our work suggests that the G* bases in these macrocyclic rings are highly dynamic.[34−36,40]

To address this G* base dynamic rotation problem, we used an approach employing carrier ligands designed to destabilize the transition state for Pt−N7 bond rotation.[34−36,40−46] We estimate that our method has led to about a billionfold decrease in the Pt−N7 rotation rate.[47,48] The G* base arrangements in the G*G* lesions can generate four conformers; recent evidence from ss models formed with d(GpG) and (less frequently) with longer oligos (see below) established that three of these conformers, HH1, HH2, and ΔHT1 (Figure 2), are common.[34−36,40,42,49] (Note that p between letters for residues is used to denote that we are referring to the d(GpG) dinucleotide or that we are drawing attention to a particular phosphodiester group in a longer oligo, e.g., for a ^{31}P NMR signal assignment.)

Some of the most revealing studies employed the chiral carrier ligand 2,2′-bipiperidine (Bip), which, when coordinated, has two energetically favored C_2-symmetrical geometries, with an *R*,*S*,*S*,*R* or *S*,*R*,*R*,*S* configuration at the asymmetric N, C, C, and N chelate ring atoms, respectively (Figure 3). The asymmetric N atoms each have an NH group fixed in a specified position and a piperidine methylene group hindering rotation by clashing with the G O6 as the base rotates toward the coordination plane. The Bip chirality influences conformer distribution and the R- or L-canting direction (Figures 2 and 3).[34,35,41] The two HH conformers, HH1 and HH2 (differing from HH1 in the direction of phosphate backbone propagation), observed for (*R*,*S*,*S*,*R*)-BipPt(d(G*pG*)) have R canting (Figure 2).[34] The HH1 and ΔHT1 conformers found for (*S*,*R*,*R*,*S*)-BipPt(d(G*pG*)) have L canting (Figures 2 and 3).[35] In both cases, only one new conformer was present. As mentioned, in later studies *three* conformers (HH1, HH2, and ΔHT1) were found to coexist when the carrier ligand lacked both chirality and NH groups, such as *N*,*N*′-dimethylpiperazine (Me$_2$ppz) and 5,5′-dimethyl-2,2′-bipyridine (5,5′-Me$_2$bipy).[36,42] Thus, both new conformers were present.

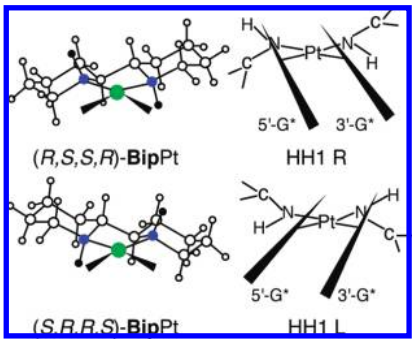

Figure 3. Left: Ball-and-stick figures of the BipPt moieties (platinum atoms are colored in green, and nitrogens are blue). The *R*,*S*,*S*,*R* and *S*,*R*,*R*,*S* configurations define the stereochemistry of the N, C, C, and N Bip ring atoms. Right: The NH and N−CH$_2$ groups of the Bip ligand are shown to illustrate how these groups influence the canting direction. G* bases are shown as triangles, with the apex of the triangle representing the five-membered ring and the base of the triangle representing the six-membered ring.

Results on d(G*pG*) models cannot help to reveal what role the 5′- and 3′-flanking residues, which can be viewed as substituents on the Pt(d(G*pG*)) macrocyclic chelate ring (Figure 1), play in dictating the underlying causes of the distortions in duplexes. Models of the type *cis*-PtA$_2$(oligo) (A$_2$ = two amines or a diamine) are needed. A study of Me$_2$ppzPt(oligo) models[40] was very informative. The 3′-X residue had no effect. As the 5′-X steric size increased, L canting of the HH1 conformer increased, but the N pucker and backbone conformation did not change. This work with L-canted models led to hypotheses concerning the probable factors in R-canted models leading to the distinctive distortions characteristic of the Lippard bp step.[40] For example, on the basis of this study and those on duplexes, we hypothesized[20,40] that perhaps minimization of steric clashes is more important than carrier-ligand hydrogen-bonding ability in explaining why anticancer activity for *cis*-PtA$_2$X$_2$-type drugs was found to decrease across the series A = NH$_3$ > RNH$_2$ > R$_2$NH.[10,50]

From the foregoing discussion, it is clear that solution studies of relatively simple nondynamic models provide valuable information on the effects of the flanking regions. Although very informative, there was no carrier-ligand NH in the Me$_2$ppzPt-(oligo) L-canted adducts.[40] Because the (*R*,*S*,*S*,*R*)-BipPt moiety has NH groups and favors the R canting found in duplexes and

(32) den Hartog, J. H. J.; Altona, C.; Chottard, J.-C.; Girault, J.-P.; Lallemand, J.-Y.; de Leeuw, F. A.; Marcelis, A. T. M.; Reedijk, J. *Nucleic Acids Res.* **1982**, *10*, 4715–4730.
(33) van Garderen, C. J.; Bloemink, M. J.; Richardson, E.; Reedijk, J. *J. Inorg. Biochem.* **1991**, *42*, 199–205.
(34) Ano, S. O.; Intini, F. P.; Natile, G.; Marzilli, L. G. *J. Am. Chem. Soc.* **1998**, *120*, 12017–12022.
(35) Marzilli, L. G.; Ano, S. O.; Intini, F. P.; Natile, G. *J. Am. Chem. Soc.* **1999**, *121*, 9133–9142.
(36) Sullivan, S. T.; Ciccarese, A.; Fanizzi, F. P.; Marzilli, L. G. *J. Am. Chem. Soc.* **2001**, *123*, 9345–9355.
(37) Williams, K. M.; Cerasino, L.; Natile, G.; Marzilli, L. G. *J. Am. Chem. Soc.* **2000**, *122*, 8021–8030.
(38) Cramer, R. E.; Dahlstrom, P. L. *J. Am. Chem. Soc.* **1979**, *101*, 3679–3681.
(39) Chottard, J. C.; Girault, J. P.; Chottard, G.; Lallemand, J. Y.; Mansuy, D. *J. Am. Chem. Soc.* **1980**, *102*, 5565–5572.
(40) Sullivan, S. T.; Saad, J. S.; Fanizzi, F. P.; Marzilli, L. G. *J. Am. Chem. Soc.* **2002**, *124*, 1558–1559.
(41) Ano, S. O.; Intini, F. P.; Natile, G.; Marzilli, L. G. *Inorg. Chem.* **1999**, *38*, 2989–2999.
(42) Bhattacharyya, D.; Marzilli, P. A.; Marzilli, L. G. *Inorg. Chem.* **2005**, *44*, 7644–7651.
(43) Sullivan, S. T.; Ciccarese, A.; Fanizzi, F. P.; Marzilli, L. G. *Inorg. Chem.* **2000**, *39*, 836–842.
(44) Wong, H. C.; Coogan, R.; Intini, F. P.; Natile, G.; Marzilli, L. G. *Inorg. Chem.* **1999**, *38*, 777–787.
(45) Wong, H. C.; Intini, F. P.; Natile, G.; Marzilli, L. G. *Inorg. Chem.* **1999**, *38*, 1006–1014.
(46) Benedetti, M.; Saad, J. S.; Marzilli, L. G.; Natile, G. *J. Chem. Soc., Dalton Trans.* **2003**, 872–879.
(47) Li, D.; Bose, R. N. *J. Chem. Soc., Chem. Commun.* **1992**, 1596–1597.
(48) Li, D.; Bose, R. N. *J. Chem. Soc., Dalton Trans.* **1994**, 3717–3721.
(49) Beljanski, V.; Villanueva, J. M.; Doetsch, P. W.; Natile, G.; Marzilli, L. G. *J. Am. Chem. Soc.* **2005**, *127*, 15833–15842.
(50) Cleare, M. J.; Hoeschele, J. D. *Bioinorg. Chem.* **1973**, *2*, 187–210.

Table 1. ^{1}H and ^{31}P NMR Signal Assignments (ppm; *J* in hertz) for the HH1 R Conformer of (*R,S,S,R*)-BipPt(oligo) Adducts[a]

	5′-G*[b]							3′-G*[b]							
adduct	H8	H1′	H2′	H2"	$J_{H1'-H2'}$/ $J_{H1'-H2''}$	H3′	H4′	H8	H1′	H2′	H2″	$J_{H1'-H2'}$/ $J_{H1'-H2''}$	H3′	H4′	^{31}P
d(G*pG*)[c]	8.76	6.32	2.48	2.73	0/6.8	4.82	4.13	8.22	6.23	2.32	2.37	9.5/4.9	4.54	4.16	−3.22
d(G*G*T)	8.77	6.33	2.46	2.73	0/7.0	4.84	4.15	8.25	6.16	2.35	2.58	9.3/4.9	4.85	4.14	−2.87
d(G*G*TTT)	8.78	6.33	2.41	2.77	0/6.9	4.89	4.03	8.24	6.08	2.30	2.53	9.6/4.7	4.87	4.06	−2.71
d(TG*G*)	8.77	6.27	2.58	2.74	0/6.8	4.91	4.27	8.67	6.24	2.48	2.41	8.7/5.6	4.56	4.20	−2.89
d(TTTG*G*)	8.76	6.28	2.60	2.76	0/7.0	4.92	4.06	8.73	6.20	2.52	2.43	8.4/5.8	4.59	4.20	−3.02
d(TG*G*T)	8.77	6.28	2.47	2.75	0/7.0	5.03	4.25	8.70	6.17	2.47	2.59	9.5/5.0	4.86	4.37	−2.75
d(pG*G*TTT)[d]	9.04	6.34	2.37	2.78	0/6.9	5.07	4.26	8.37	6.06	2.32	2.56	9.6/4.7	4.86	4.07	−2.76
d(HxapG*G*T)	8.89	6.33			0/6.7			8.59	6.16			9.3/4.8			−2.80

[a] NOESY and COSY experiments conducted at 5 or 10 °C, pH ≈ 4. [b] *anti*/*anti* conformational assignment based on the NOE cross-peaks between H8 resonances and sugar signals. [c] Reference 34. [d] At pH 7.6, the 5′-G* and 3′-G* H8 signals are at 9.32 and 8.37 ppm, respectively.

because we have studied the (*R,S,S,R*)-BipPt(d(G*pG*)) adduct containing the "unsubstituted" Pt(d(G*pG*)) macrocyclic ring,[34] we have now added 5′- and 3′-flanking residues as substituents. We chose to examine oligos with T residues because the TG*G* sequence was present in the first example of the Lippard bp step,[19] because GGT is part of the repetitive sequence found in telomeres (a potential cisplatin ss target[51−55]) and because T residues were used in the Me_2ppzPt(oligo) study.[40] The new (*R,S,S,R*)-BipPt(oligo) adducts are the first adducts with longer ss oligos shown by NMR methods to be R-canted. Furthermore, a study of 12-mers with the (*R,S,S,R*)-BipPt moiety evaluated by other methods establishes that these adducts form rather stable duplexes.[49]

Experimental Section

Materials. The (*R,S,S,R*)-BipPt$(NO_3)_2$ complex was prepared as reported.[41] Oligonucleotides, synthesized by the Microchemical Facility at Emory University, were purified by FPLC. Failed sequences were removed by using ion exchange chromatography on a Pharmacia Mono Q FPLC column (phase A = 2 M NaCl, phase B = H_2O, 0−30% phase A over ∼105 min). Collected fractions were desalted with a Pharmacia Hi-Trap desalting FPLC column (phase A = H_2O, 4.5 mL/min for 20 min), taken to dryness by rotary evaporation, and then dissolved in ∼0.5−1.0 mL of D_2O.

NMR Spectroscopy. All NMR spectra were recorded on Varian (Inova or Unity) 600 MHz instruments. A 1−1.5 s presaturation pulse was used in ^{1}H NMR collections to reduce the HOD peak, and the residual HOD signal was used to reference the spectra. ^{1}H decoupled ^{31}P NMR spectra were collected by using an 8K block size and a spectral width of ∼3000 Hz. ^{31}P NMR spectra were referenced to external trimethyl phosphate (TMP). All NMR data were processed with Felix (Molecular Simulations, Inc.).

Matrices of 512 × 2048 size were collected in nuclear Overhauser enhancement spectroscopy (NOESY) and correlation spectroscopy (COSY) experiments, conducted at 5 or 10 °C, with a spectral window of ∼6000 Hz and a presaturation pulse of ∼1 s to reduce the HOD signal. Typically, 32 scans were collected per block. A 500 ms mixing time was employed in NOESY collections. An exponential apodization function with a line broadening of 0.2 Hz and a phase-shifted 90° sine bell function were used to process the NOESY and COSY t_2 and t_1 data, respectively.

Preparation of Platinated Oligonucleotides. Typically, a sample (∼1−2 mM) of a given oligo was prepared in D_2O (∼1 mL). Oligo ε_{260} values were calculated[56] to be 30.1, 46.3, 29.1, 45.3, 37.6, 46.3, and 30.1 cm^{-1} mM^{-1} for d(GGT), d(GGTTT), d(TGG), d(TTTGG), d(TGGT), d(pGGTTT), and hexylamine-pGGT (d(HxapGGT)), respectively. The appropriate volume of an $[(R,S,S,R)\text{-BipPt}(D_2O)_2]^{2+}$ solution (∼2.5 mM) was then added to the oligo solution to give a 1:1 Pt:oligo ratio. The reaction mixture (pH ≈ 4) was kept at ∼5 °C until reaction completion. Reactions were monitored by using G* H8 NMR signals until all free oligo had been consumed; when necessary, more $[(R,S,S,R)\text{-BipPt}(D_2O)_2]^{2+}$ solution was added. After the G* H8 signals indicated complete reaction, the pH was lowered to ∼1.3−1.7. The absence of significant chemical shift changes for the G* H8 signals confirmed Pt−G N7 binding.[57,58]

Molecular Modeling. Molecular modeling and dynamics (MMD) calculations were carried out as described elsewhere.[59]

Results

Sugar proton signal assignments were based primarily on 2D NMR data; a complete explanation of these assignments (Table 1) appears in the Supporting Information. NOESY and, occasionally, COSY data were used also to assess structural features such as sugar pucker (S or N), G* nucleotide conformation (*anti* or *syn*), and the relative orientation of the two bases with respect to one another (HT or HH). For example, intraresidue H8−H3′ NOE cross-peaks are characteristically observed for N-sugars but not for S-sugars.[60] Sugar pucker conformations were also deduced from H1′ coupling patterns.[61] G* nucleotide conformations can be assessed by intraresidue H8-sugar signal NOE cross-peaks; strong H8−H2′/H2″ NOE cross-peaks and weak (or unobservable) H8−H1′ cross-peaks are characteristic of an *anti* conformation, while strong H8−H1′ NOEs are typically found for *syn* residues.[60,62,63] HH and HT base arrangements are easily distinguished through H8−H8 NOE cross-peaks; such a cross-peak is characteristic of an HH conformer, whereas the absence of such a cross-peak is indicative of an HT conformer because the H8 atoms are closer in the HH conformers than in the HT conformers.[34,35]

Residue assignments (i.e., 5′-G* vs 3′-G*) were based, when possible, on internucleotide NOEs. Internucleotide NOEs are typically observed between base proton signals and sugar

(51) Cohen, S. M.; Lippard, S. J. *Prog. Nucleic Acid Res. Mol. Biol.* **2001**, *67*, 93–130.
(52) Ishibashi, T.; Lippard, S. J. *Proc. Natl. Acad. Sci. U.S.A.* **1998**, *95*, 4219–4223.
(53) Rao, L.; Bierbach, U. *J. Am. Chem. Soc.* **2007**, *129*, 15764–15765.
(54) Ourliac, G. I.; Bombard, S. *J. Inorg. Biochem.* **2007**, *101*, 514–524.
(55) Zhang, R. G.; Zhang, R. P.; Wang, X. W.; Xie, H. *Cell Res.* **2002**, *12*, 55–62.
(56) *CRC Handbook of Biochemistry and Molecular Biology*, 3rd ed.; Fasman, G. D., Ed.; CRC Press, Inc.: Cleveland, OH, 1975; Vol. 1, Nucleic Acids.
(57) Dijt, F. J.; Canters, G. W.; den Hartog, J. H.; Marcelis, A.; Reedijk, J. *J. Am. Chem. Soc.* **1984**, *106*, 3644–3647.
(58) Qu, Y.; Farrell, N. *J. Am. Chem. Soc.* **1991**, *113*, 4851–4857.
(59) Yao, S.; Plastaras, J. P.; Marzilli, L. G. *Inorg. Chem.* **1994**, *33*, 6061–6077.
(60) Wüthrich, K. *NMR of Proteins and Nucleic Acids*; John Wiley & Sons: New York, 1986.
(61) Saenger, W. *Principles of Nucleic Acid Structure*; Springer-Verlag: New York, 1984.
(62) Kaspárková, J.; Mellish, K. J.; Qu, Y.; Brabec, V.; Farrell, N. *Biochemistry* **1996**, *35*, 16705–16713.
(63) Patel, D. J.; Kozlowski, S. A.; Nordheim, A.; Rich, A. *Proc. Natl. Acad. Sci. U.S.A.* **1982**, *79*, 1413–1417.

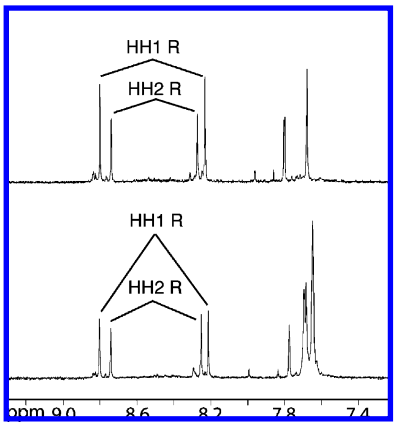

Figure 4. G* H8/T H6 region of 1D NMR spectra for (*R*,*S*,*S*,*R*)-BipPt(d(G*G*T)) (top) and (*R*,*S*,*S*,*R*)-BipPt(d(G*G*TTT)) (bottom) at equilibrium (pH ≈ 4, 23 °C). Labels mark the G* H8 signals of the conformers. Most of the minor signals are from trace impurities; the signals at ∼7.8 and 8.0 ppm are most likely from the ΔHT1 conformer, but the amount of product was too small to characterize.

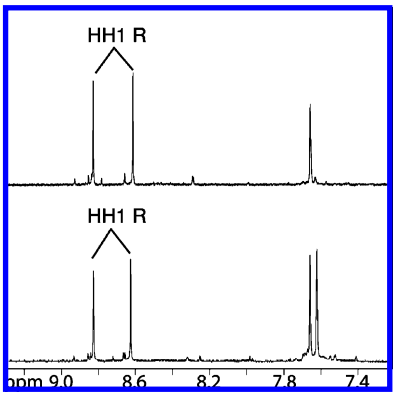

Figure 5. G* H8/T H6 region of 1D NMR spectra for (*R*,*S*,*S*,*R*)-BipPt(d(TG*G*)) (top) and (*R*,*S*,*S*,*R*)-BipPt(d(TG*G*T)) (bottom) at equilibrium (pH ≈ 4, 23 °C). Labels mark the G* H8 signals of the conformers.

resonances of the preceding residue (i.e., $(H8)_i-(H1'/H2'/H2'')_{i-1}$).[60] In other cases, assignments were based on the well-established observation that the 5′-G* sugar always adopts the N pucker, while the 3′-G* sugar has the S pucker.[34,64] In this section, for each BipPt(oligo) complex we first present ^{1}H and ^{31}P NMR features and then briefly discuss methods for conformer assignments. G H8 shifts of free oligos and a complete description of conformer assignments can be found in the Supporting Information. All solutions were at pH ≈ 4, unless otherwise noted.

(*R*,*S*,*S*,*R*)-BipPt(d(G*G*T)). Two new pairs of G* H8 signals, downfield of the H8 signals of the free d(GGT), were observed ∼30 min after initiation of the reaction. After 2 days, no free d(GGT) signals were observed, indicating complete reaction. The two new pairs of H8 signals were assigned to the HH1 R and HH2 R conformers, with a final distribution of ∼62% and ∼38%, respectively (Figure 4). The ^{31}P NMR signals (∼−3.7 to −3.9 ppm) are within the normal shift range,[29] except for two assigned as the d(G*pG*) signals of the HH1 R (−2.87 ppm) and HH2 R (−2.41 ppm) conformers (Supporting Information). Assignments were based on their relative intensities and on the characteristic shifts indicated by the (*R*,*S*,*S*,*R*)-BipPt(d(G*pG*)) analogue.[34]

(*R*,*S*,*S*,*R*)-BipPt(d(G*G*TTT)). After initiation of the reaction, two new pairs of G* H8 signals appeared downfield of the H8 signals of the free d(GGTTT), which disappeared after 2 days, indicating complete reaction. These new pairs of signals were assigned to the HH1 R and HH2 R conformers for reasons discussed below. No change in distribution of the HH1 R and HH2 R conformers (∼52% and ∼48%, respectively) was observed from the first (∼30 min) to the final spectrum (Figure 4). By analogy to (*R*,*S*,*S*,*R*)-BipPt (d(G*pG*))[34] and d(G*G*T) adducts, the ^{31}P NMR signals at −2.71 and −2.40 ppm are assigned as the d(G*pG*) signal of the HH1 R and HH2 R conformers, respectively. The d(G*pT) and d(TpT) ^{31}P NMR signals overlapped in the normal chemical shift range (∼−3.70 to −3.90 ppm).

(*R*,*S*,*S*,*R*)-BipPt(d(TG*G*)). Only one pair of new downfield G* H8 resonances was observed ∼20 min after initiation of the reaction. The free d(TGG) signals disappeared after 1 day, indicating complete reaction. The new pair of signals (Figure 5) arises from the HH1 R conformer for reasons discussed below. A ^{31}P NMR signal observed at a normal shift (−3.9 ppm) was assigned as the d(TpG*) signal,[29] while a second (at −2.89 ppm) was assigned as the d(G*pG*) signal because it has the characteristic shift for an HH d(G*pG*) cross-link.[34]

(*R*,*S*,*S*,*R*)-BipPt(d(TTTG*G*)). Only one pair of G* H8 signals, downfield of the free d(TTTGG) H8 resonances, was observed after initiation of the reaction. Reaction was complete after 24 h, as indicated by the disappearance of the free d(TTTGG) signals. The two new G* H8 signals (Supporting Information) that arise from the HH1 R conformer (see below) have a very small shift separation and even partially overlap at 5 °C. At higher temperatures, the signals disperse (Supporting Information). The ^{31}P NMR signals (∼−3.7 to −3.9 ppm) are within the normal shift range,[29] except for one at −3.02 ppm assigned as the d(G*pG*) signal, from the characteristic shift of an HH cross-link.[34]

(*R*,*S*,*S*,*R*)-BipPt(d(TG*G*T)). One pair of new G* H8 signals, downfield of the H8 signals of the free d(TGGT), was observed ∼15 min after initiation of the reaction. After ∼2 days, the reaction was complete, as indicated by the disappearance of the free d(TGGT) signals. For reasons to be discussed later, the two new signals (Figure 5) were assigned to the HH1 R conformer. The ^{31}P NMR signals (∼−3.7 to −3.9 ppm) are within the normal shift range, except for one at −2.75 ppm assigned as the d(G*pG*) signal of the HH1 R conformer because it has the characteristic shift for a phosphate group in an HH cross-link (Supporting Information).[34]

(*R*,*S*,*S*,*R*)-BipPt(d(pG*G*TTT)). Only one downfield pair of G* H8 signals was observed after ∼15 min of initiation of reaction (Figure 6); this pair is assigned to the HH1 R conformer. Free d(pGGTTT) signals disappeared after 1 h, indicating completion of the reaction. No further changes in the ^{1}H NMR spectrum occurred after 8 weeks. All ^{31}P NMR signals (∼−3.7 to −3.9 ppm) are within the normal shift range[29] except two signals observed downfield at −2.76 and −2.37 ppm. Upon increasing the pH from ∼4 to ∼7, the 5′-G* H8 signal became broad and shifted downfield by 0.27 ppm, whereas the 3′-G* H8 signal did not shift (Figure 6). Furthermore, at pH ≈ 7 the ^{31}P NMR signal at −2.37 ppm also became broad and shifted ∼2 ppm downfield; this signal is assigned to the 5′-phosphate (p) group. The signal at −2.76 ppm did not shift, assigning it to the d(G*pG*) cross-link.

(64) Sherman, S. E.; Gibson, D.; Wang, A. H.-J.; Lippard, S. J. *Science* **1985**, *230*, 412–417.

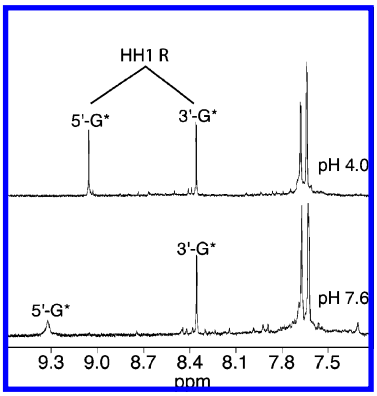

Figure 6. G* H8/T H6 region of 1D NMR spectra for (*R*,*S*,*S*,*R*)-BipPt(d(pG*G*TTT)) at equilibrium (23 °C) and different pH values. Labels mark the G* H8 signals of the conformers.

(*R*,*S*,*S*,*R*)-BipPt(d(HxapG*G*T)). To examine whether the presence of a 5′-flanking residue that is bulkier than a phosphate group has a significant effect on conformer distribution and canting, we used a modified pGGT oligo with a hexylamine group covalently attached to the phosphate group. The 1D NMR spectrum collected on this adduct ∼15 min after initiation of the reaction shows only one pair of new G* H8 signals, downfield of the H8 signals of the free oligo. After ∼1 day, the reaction was complete, as indicated by the disappearance of the free d(HxapGGT) signals (Supporting Information). The product has one ^{31}P NMR signal (−3.8 ppm) with a normal shift[29] and is assigned to d(G*pT). A ^{31}P NMR signal at −2.33 ppm is assigned to Hxap because it has the same shift as this group of the free d(HxapGGT) (Supporting Information). The ^{31}P NMR signal at −2.80 is assigned to d(G*pG*). Because it has the characteristic shift for a d(G*pG*) group in an HH cross-link[34] and is similar to the d(G*pG*) shift of the HH1 R conformer of the adducts discussed above, we conclude that this is an HH1 R conformer.

Conformer Assignments. As mentioned above, the conformation of each species was assigned on the basis of a number of features found previously for *cis*-PtA_2(oligo) conformers. For example, the HH conformers show the following: (a) downfield H8 and ^{31}P NMR signals,[25,28,29,31,32,34,65,66] (b) H8−H8 NOEs,[13,28,34−36] and (c) two weak or no H8−H1′ cross-peaks, indicating that both G* residues have an *anti* conformation.[25,34] Because the two possible HH conformers, HH1 or HH2, differ only in the direction of phosphate diester backbone propagation,[34] they exhibit few spectral differences. The initial discovery of the HH2 conformer involved the (*R*,*S*,*S*,*R*)-BipPt(d(G*pG*)) adduct;[34] the difference in the residue with the canted base provided a clear way to distinguish the HH1 conformer from the HH2 conformer. Another useful difference between the HH conformers is the absence of any observable H8-sugar NOE cross-peaks for the 3′-G* of the HH2 conformer, whereas the HH1 conformer has such cross-peaks.[34] This difference was used to distinguish between the HH1 and HH2 conformers of Me_2ppzPt(d(G*pG*)).[36] HH conformers are clearly different from the ΔHT1 conformer, which typically exhibits the following spectral characteristics: (a) upfield H8 and ^{31}P NMR signals; (b) no H8−H8 NOE; (c) one weak or absent H8−H1′ cross-peak; (d) one strong H8−H1′ cross-peak, indicating a *syn* 3′-G* residue.[35−37] Another possible HT conformer, ΛHT2, appears to be unstable and has not yet been reported to be abundant in any adduct.[35]

Discussion

When compared to the parent DNA, the formation of an intrastrand N7−Pt−N7 G*G* cross-link introduces additional new stereochemistry and (at least in duplexes) increases the dynamic nature of the DNA. Efforts to define the structure of DNA bearing a cross-link have been hampered by the increased dynamic motion of the adducts.[14] DNA with ss character is likely to be present during breathing motions of duplex DNA bearing the cross-link adduct. Single-strand DNA exists in telomeres and also in the normal course of DNA biochemistry. Also, understanding ss adducts may eventually prove to be of direct importance in assessing the structure and mechanism of Pt-containing antisense oligo drugs.[6,67,68] However, the more immediate relevance of the current work is the assessment of the possible role of the right-handed HH1 cross-link in influencing the distortions in DNA duplexes, especially the factors contributing to the unusually large positive slide and shift of the 5′-XG* bp step. The most abundant long-lived conformer observed for all (*R*,*S*,*S*,*R*)-BipPt(oligo) adducts studied here is the right-handed HH1 conformer. These right-handed adducts are unlike Me_2ppzPt(oligo) adducts and previously studied ss adducts, including those formed by anticancer drugs,[40] which are left-handed. Prior to discussing effects in the 5′ direction, we discuss the absence of any effects in the 3′ direction.

*Note: Henceforth, we shall use a shorthand notation to designate the HH1 R conformer of (R,S,S,R)-BipPt(oligo) adducts. Thus, the (R,S,S,R)-BipPt(d(TG*G*T)) adduct is designated simply as d(TG*G*T).*

Lack of Influence of 3′-Substituents on Conformer Stability, on G* Base Canting, and on G* H8 Shifts. For the (*R*,*S*,*S*,*R*)-BipPt(d(G*pG*)) adduct, the HH1 R conformer (55%) is only slightly more abundant than the HH2 R conformer (45%). This relationship is almost unaffected in the (*R*,*S*,*S*,*R*)-BipPt(oligo) adducts with only a 3′-flanking residue, regardless of the size of the 3′-residue. This finding that a 3′-substituent has little effect on conformer stability relative to the d(G*pG*) adduct in a right-handed adduct can be attributed to the long distance of the 3′-substituent from the carrier ligand (Figure 7).

The G* H8 shifts of the HH1 R conformer of (*R*,*S*,*S*,*R*)-BipPt(oligo) complexes with a residue flanking only a 3′-substituent are almost identical to those found for the (*R*,*S*,*S*,*R*)-BipPt(d(G*pG*)) adduct[34] (Table 1). Thus, G* base canting is not influenced by the presence of one or more 3′-flanking T residues. The observations agree well with the previous finding that the 3′-T had no influence on the H8 shifts of the left-handed Me_2ppzPt(d(G*G*T)) adduct.[40] A 3′-phosphodiester group is too far from the G* H8 atom (Figure 7) to have much direct influence on the H8 shift. Thus, our results show that a 3′-residue exerts no significant effect on shift, on the direction or degree of canting, and on conformer stability even for right-handed adducts in which the carrier ligand has both bulk and an NH group.

(65) Mukundan, S., Jr.; Xu, Y.; Zon, G.; Marzilli, L. G. *J. Am. Chem. Soc.* **1991**, *113*, 3021–3027.
(66) van der Veer, J. L.; van der Marel, G. A.; van den Elst, H.; Reedijk, J. *Inorg. Chem.* **1987**, *26*, 2272–2275.
(67) Berghoff, U.; Schmidt, K.; Janik, M.; Schröder, G.; Lippert, B. *Inorg. Chim. Acta* **1998**, *269*, 135–142.
(68) Janik, M. B. L.; Lippert, B. *J. Biol. Inorg. Chem.* **1999**, *4*, 645–653.

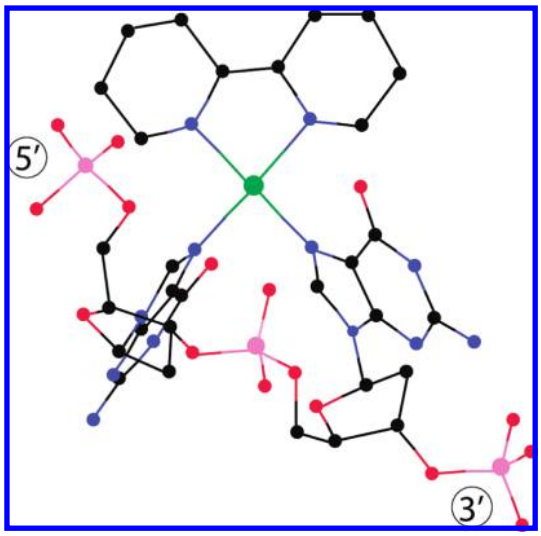

Figure 7. Ball-and-stick figure showing the macrocyclic chelate ring of (*R*,*S*,*S*,*R*)-BipPt(d(pG*pG*p)) from a MMD-minimized HH1 R model of the d(TG*G*T) adduct. [In this depiction, all hydrogen atoms are omitted for clarity and the atoms are color coded as follows: platinum, green; phosphorus, pink; nitrogen, blue; oxygen, red; and carbon, black.]

Dramatic Influence of 5′-Substituents on Conformer Stability. In sharp contrast to the negligible effect of 3′-substituents on conformer distribution of the (*R*,*S*,*S*,*R*)-BipPt(oligo) adducts compared to that of the (*R*,*S*,*S*,*R*)-BipPt(d(G*pG*)) adduct, the HH1 R conformer was the only identifiable conformer observed for (*R*,*S*,*S*,*R*)-BipPt(oligo) adducts with a 5′-substituent, regardless of whether this substituent is T, TTT, Hxap, or simply one phosphate group. Again, it is clear from our experimental data and from our previous work that this 5′-substituent effect is operative in cases where the adduct is right-handed or left-handed or where the carrier ligand either has or does not have an NH group. As shown in Figure 7, a 5′-substituent is closer to the carrier ligand than a 3′-substituent. Because of the importance of the right-handed canting, we examined in depth the 5′-substituent effect on canting and on backbone structure.

Influence of 5′-Substituents on G* Base Canting and H8 Shifts. Because of the dependence of canting on the 5′-substituent, we discuss in more depth the relationship of H8 shifts to canting. The G* H8 signal is generally a good probe for assessing the direction (R or L, Figure 2) and the orientation (H8-in or H8-out) of base canting.[14,26] Because the degree of canting is much greater for H8-in than for H8-out, we can refer to the two as canted and uncanted (or less canted) bases, respectively. In a typical canted G* base, the H8 atom is positioned toward the *cis*-G*. The ring-current anisotropy of this *cis*-G* base causes an upfield shift of the H8 signal of the canted G*. In a less canted orientation, the H8 atom is positioned away from the *cis*-G* base.[26] The H8 atom of a less canted G* may experience deshielding by the magnetic anisotropy of the Pt atom and possibly of the canted *cis*-G*.[69−71] Typically, canted and less canted bases of *cis*-PtA_2(d(G*pG*)) adducts have H8 shifts of ∼7.8−8.3 and ∼8.7−9.2 ppm, respectively.[35] For (*R*,*S*,*S*,*R*)-BipPt(d(G*pG*)), the 3′-G* base is canted for the HH1 R conformer (upfield 3′-G* H8 signal) (Table 1).[34] Clockwise rotation of bases decreases the extent of R canting, eventually leading to an L-canted conformer.

To assess the influence of the 5′-flanking nucleotide chain (T or TTT) on the structure (e.g., base canting, backbone structure), we must factor out the possible through-space anisotropic and through-bond inductive effects of such residues on the G* H8 and sugar proton NMR shifts compared to the shifts of the unsubstituted (*R*,*S*,*S*,*R*)-BipPt(d(G*pG*)) parent (Table 1). Our analysis of shifts indicates that changes in canting within the range estimated for the adducts in this study will have little effect on 5′-G* H8 shifts but large effects on 3′-G* H8 shifts. For adducts in the current study, we find very little change in the 5′-G* H8 shifts (Figure 8). Our analysis also indicates that the through-space deshielding effects of the phosphodiester groups are small but that the effects of the 5′-p group on the 5′-G* H8 shift can be large (see below).

G* Base Canting in (*R*,*S*,*S*,*R*)-BipPt(d(TG*G*)) and (*R*,*S*,*S*,*R*)-BipPt(d(TG*G*T)) Adducts. The 5′-G* H8 signals for d(TG*G*) and d(TG*G*T) have almost the same shift as the 5′-G* H8 signal of d(G*pG*) and several other adducts (Table 1 and Figure 8). In contrast, the differences in 3′-G* H8 shifts from d(G*pG*) to d(TG*G*) and d(TG*G*T) are significant (∼0.45 ppm downfield). An anisotropic deshielding effect of the phosphodiester or the thymidine moieties of the 5′-T residue cannot be so large as to be responsible for the dramatic shift difference of the 3′-G* H8 signal because the signal of the much closer 5′-G* H8 atom is almost unchanged. Thus, without question, the addition of a 5′-T residue causes the 3′-G* base to rotate clockwise.

The similarity in shifts of the respective G* H8 signals of the HH1 R conformer of the d(TG*G*) and d(TG*G*T) models (Table 1) is consistent with the conclusion that the 5′-substituent is the key factor in influencing base canting (which in turn influences the H8 shifts of the cross-link moiety) and that the 3′-substituent has little influence on canting. Thus, we focus next on estimating the changes in G* base canting caused by the 5′-T flanking residue.

To interpret the effect of the 5′-T on G* base canting, we examined which canting changes could explain the negligible differences in the 5′-G* H8 shift and the large difference in the 3′-G* H8 shift. We tested whether the ring current anisotropy of the G* bases would explain the results. Our procedure for calculating the effect of the G* anisotropy on the H8 shifts is described briefly here, and some details are presented in the Supporting Information. We began with molecule R1 of *cis*-$Pt(NH_3)_2$(d(pG*pG*)) (cf. Figure 1, an R-canted molecule characterized by X-ray crystallography).[12] This selection allowed us to use well-defined bond lengths and angles, etc. We then replaced the *cis*-$Pt(NH_3)_2$ moiety with (*R*,*S*,*S*,*R*)-BipPt. Next, the C5−N7−Pt−*cis*-N torsion angle of each base-in R1 was changed to make the bases perpendicular to the coordination plane (i.e., uncanted bases, Supporting Information). We calculated the effect on the shift caused by the ring current anisotropy of one *cis*-G* base on the H8 shift of the other G* base by using methods described elsewhere.[72,73] The calculations show no ring current shift effect (i.e., 0 ppm) on the 5′-G* and 3′-G* H8 signals when both of the G* bases of (*R*,*S*,*S*,*R*)-BipPt(d(G*pG*)) are uncanted (respective C5−N7−Pt−*cis*-N torsion angles of ∼90° and ∼−90°, structure not shown).

(69) Carlone, M.; Fanizzi, F. P.; Intini, F. P.; Margiotta, N.; Marzilli, L. G.; Natile, G. *Inorg. Chem.* **2000**, *39*, 634–641.
(70) Elizondo-Riojas, M.-A.; Kozelka, J. *Inorg. Chim. Acta* **2000**, *297*, 417–420.
(71) Sundquist, W. I.; Bancroft, D. P.; Lippard, S. J. *J. Am. Chem. Soc.* **1990**, *112*, 1590–1596.
(72) Case, D. A. *J. Biomol. NMR* **1995**, *6*, 341–346.
(73) Giessner-Prettre, C.; Pullman, B. *Biopolymers* **1976**, *15*, 2277–2286.

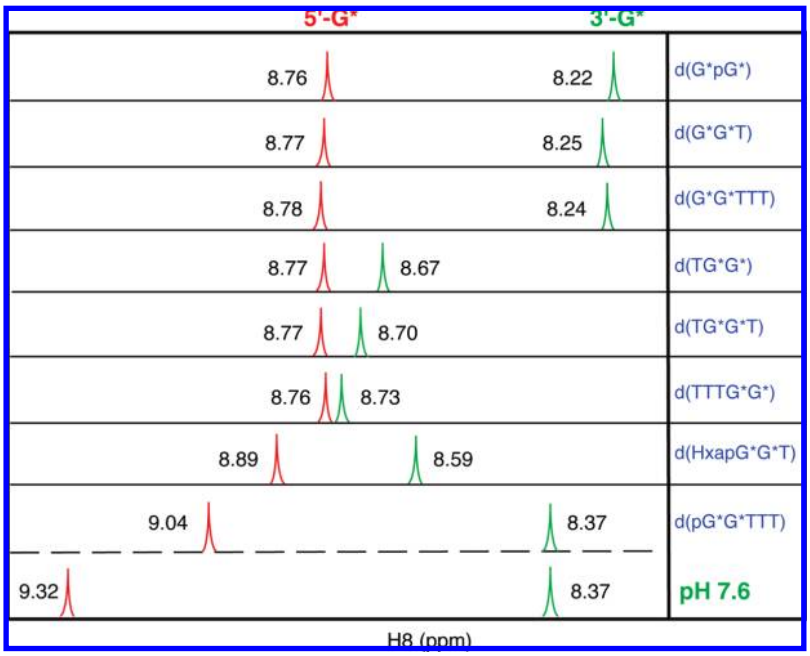

Figure 8. Comparison of 5′-G* and 3′-G* H8 shifts of the HH1 R conformer for all (*R*,*S*,*S*,*R*)-BipPt(oligo) adducts at 5 °C and pH ≈ 4.

Finally, we systematically evaluated G* H8 shift changes caused by many different combinations of torsion angles.

In this way, we determined which combinations of d(G*pG*) and d(TG*G*) structures could account for the shift differences observed (Supporting Information). One starting d(G*pG*) structure (**4**; Figure S9) with C5−N7−Pt−*cis*-N torsion angles of ca. 90° and ca. −50° for the 5′-G* and the 3′-G* bases, respectively, could account for the effect of a 5′-T only if the 5′-G* base in the d(TG*G*) analogue had rotated clockwise (final torsion angle ∼55°; H8 moves toward the 3′-G* base). However, the H8−H8 separation of this "base-in" d(TG*G*) structure (**3**; Figure S9) was very short (1.6 Å).

To assess how reasonable the short H8−H8 separation was, we compared the relative H8−H8 and T Me−H6 NOE cross-peak volumes of the d(TG*G*) adduct and of the d(G*G*T) adduct, which has H8 shifts (Table 1) and hence canting very similar to that of the d(G*pG*) adduct. (The T Me−H6 distance is the same in both adducts.) Figures 4 and 5 show the ^{1}H NMR spectra of the samples used for NOESY experiments at 5 °C and pH ≈ 4. For d(G*G*T), the T H6−CH_3:G* H8−G* H8 volume ratio is ∼1.5, while for d(TG*G*), the T H6−CH_3:G* H8−G* H8 volume ratio is ∼1.9. The H8−H8 volume was lower for the d(TG*G*) adduct, indicating that the addition of a 5′-T should lead to a d(TG*G*) structure with a H8−H8 distance longer than that in the d(G*pG*) structure. However, the base-in d(TG*G*) structure **3** (Figure S9 in the Supporting Information) has a very short H8−H8 distance; we thus ruled out this structure. Because the d(G*pG*) structure **4** (Figure S9) is reasonable only if the d(TG*G*) structure **3** is formed, we can also rule out structure **4**.

Two other combinations, d(TG*G*) structure **2** in combination with d(G*pG*) structure **1** and with d(G*pG*) structure **5**, are feasible on the basis of shift changes. In Figure 9, we illustrate the most likely one of these two combinations, d(G*pG*) structure **1** (left) with d(TG*G*) structure **2** (right). This combination of structures predicts that the addition of a 5′-T causes a slight increase in the H8−H8 distance, and the other combination predicts a slight decrease in this distance.

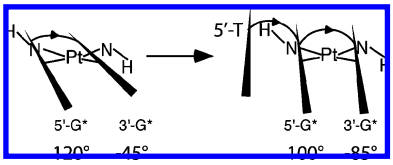

Figure 9. Change in canting when a 5′-T is present relative to the (*R*,*S*,*S*,*R*)-BipPt(d(G*pG*)) complex. Torsion angles are provided for the bases in the R-canted starting structure (left) and the low-canted final structure (right). Because the angles are defined with the *cis*-N, a clockwise rotation causes the 5′-G* value to decrease and the 3′-G* absolute value to increase. The NH groups of the (*R*,*S*,*S*,*R*)-Bip ligand are shown.

Because the NOE volume data indicate that this distance increases, the torsion angles shown in Figure 9 are most consistent with the data. This analysis indicates that the addition of a 5′-T residue causes both bases to rotate clockwise. As a result, the canting degree decreases, but the canting remains R. We refer to this structure as the "low-canted" HH1 R conformer. Of some note, although we used the R1 X-ray structure mainly to define structural features such as bond lengths and we did not use the R1 C5−N7−Pt−*cis*-N torsion angles, the respective 5′-G* and 3′-G* torsion angles for the best structure we calculated (ca. 100° and ca. −85°) are very similar to those of R1 (ca. 97° and ca. −86°).[12]

(*R*,*S*,*S*,*R*)-BipPt(d(TTTG*G*)). The d(TTTG*G*) 5′-G* and 3′-G* H8 signals have shifts similar to those of the d(TG*G*) signals (Table 1 and Figure 8). The d(TTTG*G*) 3′-G* H8 signal is only 0.06 ppm downfield, an indication that the larger chain (5′-TTT vs 5′-T) causes some further slight decrease in the degree of R canting. Nevertheless, the size of the flanking region is of secondary importance. Relative to the d(G*pG*) adduct, the most evident structural change caused by either the 5′-TTT or 5′-T substituent is a decrease in canting of both G* bases, leading to a low-canted right-handed HH1 R conformer (Figure 9).

(*R*,*S*,*S*,*R*)-BipPt(d(HxapG*G*T)): Implications for the Magnetic Anisotropic Effects of a 5′-T Residue. Clearly, a 5′-substituent as small as one T residue can play a major role in influencing canting. Therefore, we examined d(HxapG*G*T)

to assess the influence on base canting of a group smaller than a 5′-T residue but still linked to the 5′-G* via a phosphodiester group. The Hxap substituent also allowed us to evaluate anisotropic effects of the 5′-T residue.

For the d(HxapG*G*T) adduct, the G* H8 shifts have values similar to those found for adducts with a 5′-T substituent (Figure 8 and Table 1). The 3′-G* H8 signal is shifted slightly less vs the d(G*pG*) adduct than found for the d(TG*G*) adduct, indicating that the 5′-Hxap group has an effect similar to but slightly less than that of 5′-T in inducing a decrease in the canting.

Nevertheless, the 5′-G* H8 shift (which is insensitive to canting) of the d(HxapG*G*T) adduct is ∼0.1 ppm downfield from the shift characteristic for adducts with 5′-T and 5′-TTT groups. It is reasonable to suggest that the TpG* phosphodiester group also has an effect similar to that of Hxap. The absence of an effect of the 5′-T residue on the 5′-G* H8 shift relative to adducts with no 5′-flanking residue can be attributed to the T base ring current causing an upfield shift of ∼0.1 ppm. The deshielding TpG* phosphodiester group and the shielding T base cancel, explaining the absence of any effect by the 5′-T and 5′-TTT substituents. This conclusion is supported by the effects found on raising the temperature (Supporting Information). At 50 °C, the H8 signals of adducts with a 5′-T have shifts very similar to those of the d(HxapG*G*T) adduct at 5 °C. We attribute this result at 50 °C to unstacking and enhanced dynamic motion of the 5′-T residue; unstacking decreases the steric effect of the larger 5′-T group on canting, and the increased dynamic motion averages the 5′-T base magnetic anisotropic shielding to near zero.

(*R*,*S*,*S*,*R*)-BipPt(d(pG*G*TTT)) Canting. For the d(pG*G*TTT) adduct, we confine our initial discussion to 3′-G* base canting. The 3′-G* H8 signal is only slightly downfield (0.15 ppm) compared to that of analogues lacking a 5′-substituent, for example, d(G*G*TTT) (Figure 8). Thus, the 5′-p group has just a small ability to lower the degree of 3′-G* base canting. As documented above, the (*R*,*S*,*S*,*R*)-BipPt(oligo) adducts with larger 5′-substituents have 3′-G* H8 signals with ∼0.5 ppm shift differences, which reflect decreases in canting. The canting calculated by using the 3′-G* H8 shift of the d(pG*G*TTT) adduct is intermediate between the no-substituent and the 5′-residue adduct types (Supporting Information). For Me_2ppzPt-(oligo) adducts, the shift of the remote 3′-G* H8 atom was also useful for assessing the degree of canting.[40] For these adducts, in which H-bonding is not possible because no carrier-ligand NH is present, the 5′-substituent effect must be caused by steric clashes. The steric effect of the 5′-p group in Me_2ppzPt-(d(pG*pG*)) was smaller than that of the 5′-T residue in Me_2ppzPt(d(TG*G*)). Thus, the smaller steric bulk of the 5′-p group vs the complete 5′-nucleotide for d(pG*G*TTT) explains the smaller decrease in 3′-G* base canting caused by the 5′-p group than the decrease caused by a complete nucleotide.

(*R*,*S*,*S*,*R*)-BipPt(d(pG*G*TTT)): Anisotropic Effects and Hydrogen Bonding of the 5′-Flanking Phosphate Group. The 5′-G* H8 shift of the d(pG*G*TTT) adduct is noteworthy in that this signal for an adduct with a protonated 5′-p is considerably more downfield (0.27 ppm) at pH ≈ 4 than this signal for adducts with a 5′-T. The calculations based on canting suggest that this 5′-G* H8 signal will experience a ca. 0.03 ppm *upfield* shift because of G* base anisotropy (Supporting Information). To identify the cause of the high deshielding effect on the 5′-G* H8 signal of a protonated 5′-p, we assessed our past model data and conducted several studies.

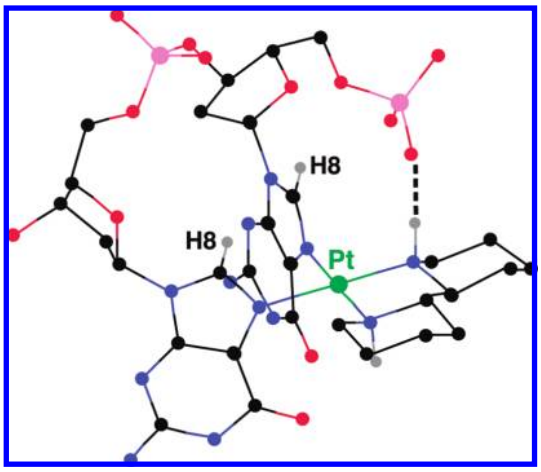

Figure 10. Ball-and-stick minimized MMD HH1 R model of (*R*,*S*,*S*,*R*)-BipPt(d(pG*pG*)). The dashed line indicates the H-bonding between the protonated 5′-p group and Bip(NH). [In this depiction, all hydrogen atoms, except the G* H8 and Bip(NH) atoms, are omitted for clarity. The atoms are color coded as follows: platinum, green; phosphorus, pink; nitrogen, blue; oxygen, red; carbon, black; and hydrogen, gray.]

Examining our past model studies, we note that the effect of a protonated 5′-p of Me_2ppzPt(d(pG*pG*)) is to shift the 5′-G* H8 only ∼0.1 ppm downfield of that for Me_2ppzPt-(d(TG*G*)).[40] This result strongly indicates that the anisotropic effect of the protonated 5′-p group on the 5′-G* H8 shift is not very different from that of a phosphodiester group. Because the protonated 5′-p group deshields the 5′-G* H8 signal more (0.27 ppm) for (*R*,*S*,*S*,*R*)-BipPt(d(pG*G*TTT)) than the ∼0.1 ppm deshielding of this signal for Me_2ppzPt(d(pG*pG*)),[40] we conclude that the 5′-p group is closer to the 5′-G* H8 atom in the (*R*,*S*,*S*,*R*)-BipPt adduct and that this proximity causes the higher deshielding. We further hypothesize that the proximity is a result of the fact that the 5′-p is hydrogen-bonded to a Bip(NH) group. Our MMD calculations on (*R*,*S*,*S*,*R*)-BipPt(d(pG*pG*)) revealed that, in a minimized HH1 R model, the 5′-p is positioned on the same side of the Bip ligand as the NH group; the Bip(N)−5′-p(O) distance is 2.8 Å, consistent with H-bonding (Figure 10).

Next we studied the pH dependence of the H8 signals for (*R*,*S*,*S*,*R*)-BipPt(d(pG*G*TTT)). When the pH was increased from ∼4 to ∼7, the 5′-G* H8 signal shifted even further downfield (to 9.32 ppm, Figure 8); the 3′-G* H8 signal did not shift, consistent with no change in canting. The deshielding effect of the deprotonated 5′-p group on the 5′-G* H8 signal for d(pG*G*TTT) is large, ∼0.5 ppm (based on the shift of this signal for adducts of oligos lacking a 5′-substituent or having a 5′-T). The very downfield H8 shift for simple *cis*-A_2Pt(5′-$GMP)_2$ models when the phosphate groups are deprotonated[74] is caused by a combination of a high anisotropy and a strong H-bonding ability of this 5′-group. This combination also explains the very downfield shift position for the 5′-G* H8 signal for d(pG*G*TTT) when the 5′-p group is deprotonated. Similarly, H-bonding/deshielding by the phosphate group upon deprotonation accounts for the very downfield shift of the 5′-G* H8 signal of all *cis*-A_2Pt(oligo) complexes with a 5′-p group studied in this way; these adducts all had primary or secondary amine groups for which the H-bonding between the 5′-p group and the carrier-ligand amine group is possible.[25,29,33]

(74) Saad, J. S.; Scarcia, T.; Natile, G.; Marzilli, L. G. *Inorg. Chem.* **2002**, *41*, 4923–4935.

Backbone. For all (*R*,*S*,*S*,*R*)-BipPt(oligo) adducts with a 5′-flanking nucleotide, the sugar moiety of the 5′-G* residue has the N pucker conformation, as found universally for *cis*-A_2Pt intrastrand cross-link adducts of both ss and duplex DNA.[20,24,34−36,65,66] The 3′-G* in adducts retains the S pucker conformation favored by B-DNA in all these same types of cross-links.

A striking feature of the G*G* sugar signals of (*R*,*S*,*S*,*R*)-BipPt(oligo) adducts is that the couplings and shifts of the HH1 conformer are very similar (Table 1). These results strongly indicate that even a 5′-residue, although positioned close to the G*G* lesion, causes no detectable changes in backbone geometry, consistent with the X-ray findings[12,19,27] and our findings on Me_2ppzPt(oligo) ss adducts.[40] Although ^{31}P NMR shifts are difficult to interpret, they are sensitive to the backbone structure. As shown in Table 1, ^{31}P NMR shifts are relatively insensitive to the presence of a 5′-substituent, suggesting again that the backbone favors a particular structure. Furthermore, the backbone is not affected by the strong 5′-p(O)−(NH)Bip H-bonding in the (*R*,*S*,*S*,*R*)-BipPt(d(pG*G*TTT)) adduct. For example, the 5′-G* $J_{H1'-H2'}$/$J_{H1'-H2''}$ coupling is 0/6.5 Hz at pH 7.6 vs typical values of 0/6.9 Hz for other adducts, and the 3′-G* $J_{H1'-H2'}$/$J_{H1'-H2''}$ coupling is 9.7/4.5 Hz vs typical values of 9.3/5.0 Hz. The G*pG* ^{31}P NMR signal for d(pG*G*TTT) does not shift upon phosphate deprotonation; this result provides further evidence that the structure of the cross-link moiety is not affected by the stronger 5′-p−Bip(NH) H-bonding.

Interrelation of the 5′-Residue Position and Canting. Although the 3′- and 5′-substituents do not change the relatively fixed structure of the backbone within the macrocyclic ring for a given conformer, the 5′-substituent has a dominant influence on both conformer stability and canting. Thus, it is important to identify the underlying reasons for the effects of the 5′-substituent. The results described above clearly show that the larger 5′-substituents have the greater effects. This trend hints at steric effects. These can be manifest purely as repulsive nonbonded interactions. Alternatively, the steric clashes either can be enhanced by H-bonding or can weaken H-bonding.

We previously considered the role of the carrier ligand in repositioning of the 5′-X residue.[40] As can be seen from Figure 1 (top) and Figures 7, 10, and S11 (Supporting Information), either one NH_3 or half of the Bip ligand is close to the 5′-flanking residue. Carrier-ligand NH H-bonding of the XpG* phosphate group appeared to be weak or possibly absent in the X-ray and NMR structures with the Lippard bp step.[19,20] The X-ray structure of *cis*-Pt(NH_3)$_2$(d(pG*pG*)) has R molecules with the 5′-p group at a similar "intermediate" distance.[12] At the time it was not clear whether the repositioning was the result of the need for separation of the 5′-X residue from the carrier ligand to avoid steric clashes or the result of the demands of the cross-link structural features (X•X′ WC base pairing, unstacked bases of the two G* residues, and N pucker of the 5′-G*). The most likely alternative carrier-ligand interaction repositioning the 5′-X residue would be steric clashes between the part of carrier ligands *cis* to the 5′-G* and the 5′-X residue. It was conceivable that the R canting itself, induced by other structural features in duplexes, causes the characteristic changes in the 5′-X residue. This possibility led us to investigate the unique (*R*,*S*,*S*,*R*)-BipPt(oligo) HH1 R ss models reported here, in which the R canting is dictated by the Bip carrier ligand and not by the presence of a duplex.

We conducted MMD calculations on an (*R*,*S*,*S*,*R*)-BipPt(d(TG*G*)) HH1 R model to assess the position of the TpG* phosphodiester group and the possible H-bonding of this group with Bip(NH). The minimum-energy HH1 R model has a relatively longer 5′-p(O)−(N)Bip distance (2.92 Å) than for the (*R*,*S*,*S*,*R*)-BipPt(d(pG*pG*)) model (2.80 Å) described above. In this d(TG*G*) model, some torsion angles of the TpG* phosphodiester group distort to allow this weaker H-bonding to occur. In the d(pG*pG*) model, these torsion angles have normal values. Our experimental data indicate that such a distortion is unlikely to be present. For example, the TpG* ^{31}P NMR shift (ca. −3.9 ppm) for d(TG*G*) is normal. Thus, the calculations indicate that while H-bonding between the TpG* phosphodiester group and the Bip(NH) is possible, it is likely to be weak.

To complement the MMD calculation and to simulate interactions in a duplex, we also used our previous graphics approach, which involves constructing hybrid structures from pieces of known structures.[40] Beginning with a cisplatin 9-mer model with a d(CG*G*C) sequence,[20] we constructed a d(TG*G*T) hybrid model by replacement of the NH_3 ligands with (*R*,*S*,*S*,*R*)-Bip, and C residues with T residues. In this hybrid structure with the 5′-T residue having an N pucker and the P−O3′−C3′−C4′ torsion angle (ε) having the 180° value of the 9-mer (Supporting Information), steric clashes between the (*R*,*S*,*S*,*R*)-Bip ligand and the flanking residues appear to be minimal. It is obvious that the features of the Lippard bp step place the 5′-T in a position where there are almost no clashes, even with a carrier ligand having (*R*,*S*,*S*,*R*)-Bip bulk. Modifying this (*R*,*S*,*S*,*R*)-BipPt(d(TG*G*T)) molecule to have a B-form ε value (155°) gives a hybrid structure with a clash between the 5′-T H2′ atom and the Bip H on the C_α *syn* to the NH. However, no clashes result when the ε value is changed to that of the L-canted *cis*-Pt(NH_3)$_2$(d(CG*G*)) complex (−146°).[27] If the 5′-X sugar pucker is changed to S (ε remains 180°), small (*R*,*S*,*S*,*R*)-Bip−5′-T steric clashes are evident. Furthermore, if the 5′-X residue has S pucker and the ε value (−146°) of the *cis*-Pt(NH_3)$_2$(d(CG*G*)) structure,[27] no (*R*,*S*,*S*,*R*)-Bip−5′-T steric clashes do occur. In contrast, if the 5′-X residue has an S-sugar pucker and the ε value of B-DNA (155°), clear (*R*,*S*,*S*,*R*)-Bip−5′-X steric clashes do occur.

Integration of Results from Duplex and ss Models. These considerations indicate that the positioning of the 5′-residue as found in duplexes with the Lippard bp step minimizes steric clashes. Both this modeling and our experimental results indicate that the right-handed cross-link has clashes with the 5′-residue. Our results suggest that if the distortion characteristic of the Lippard bp step did not occur, there would be severe clashes with the carrier ligand. If the 5′-residue moves to decrease the clashes, the resulting changes both in position and in sugar pucker minimize the steric interaction with the carrier ligand such as to possibly allow weak H-bonding. In ss adducts, the clashes can be decreased by changing the R canting toward L canting. For example, all three molecules in the X-ray structure of *cis*-Pt(NH_3)$_2$(d(CG*G*)) are highly L-canted, the ε value is within the normal range (−146°), and the sugar pucker of the C residue maintains the S character.[27] As described previously,[40] these features are needed to minimize steric clashes between the 5′-C and 5′-G* residues. However, it is reasonable to postulate that L canting is not structurally feasible in a cross-link within a duplex. As a result, the rather unexpected and unforeseen Lippard bp step distortion occurs. This distortion

must be an energetic compromise, driven by the strong bonding between Pt and the N7 of the guanine base. The distortion was not revealed by computations, even computations with restraints from NMR data, because the distortion is ordinarily not favorable and therefore "minimization of energy" employing typical force fields will not discover the Lippard bp step. In the absence of this feature, the features of the G*G* cross-link itself also elude complete clarification by computational and NMR methods.

Our interpretation downplaying the role of the carrier-ligand NH H-bonding is controversial. This H-bonding concept is appealing, and there is little doubt that under favorable situations H-bonding to the 5′-X residue can occur because, as shown in Figure 7, these groups are necessarily close. When the carrier ligand has at least two protons on a given nitrogen (primary amine or NH_3), then of necessity a H-bond-accepting group on a *cis*-G ligand must be close enough to the NH to benefit energetically from adventitious H-bond formation. The main stabilizing interaction is the Pt−N7 bond. Thus, a better test of the importance of H-bonding is to assess conformations of adducts in which the amine has only one NH. In these cases, the Pt−N7 bond does not necessarily juxtapose a G ligand H-bond acceptor near an NH group. We note, with some emphasis, that the studies we have performed to assess the conformation of G adducts in solution invariably show that conformers in which H-bonding would be possible are less stable than other conformers for which such H-bonding is not possible.[36,40,69,75−77] In particular, the O6 of guanine does not seem to compete as well as water for accepting a H-bond from the Pt−NH group, and thus conformers with this group H-bonded to water are favored over conformers with this group H-bonded to O6. These studies were conducted with G bound as a monodentate ligand, and the base is able to rotate to assume the preferred orientation. When a sugar phosphodiester backbone links the two Pt-bound G bases, many other factors enter into the presence or absence of a H-bond.

The present study shows that if the H-bond-accepting group is oxygen of a deprotonated 5′-phosphate group, then strong H-bonding does occur and an R-canted HH1 structure is favored. However, the 5′-phosphate group is both sterically relatively small and an excellent H-bond acceptor. In contrast, the phosphodiester group is a weaker acceptor and sterically bulkier. Thus, we offer the suggestion that H-bond formation between Pt−NH and phosphodiester (XpG*) groups is not strong enough to drive a particular structure and that any such H-bonding present in duplexes results mostly from adventitious juxtapositioning of these groups. Certainly, all the evidence points to the need for strong interactions to drive the distortion we refer to as that of the Lippard bp step. Several other results leave little doubt that steric effects can be solely responsible for the Lippard bp step feature. In particular, we note that Me_2ppzPt(oligo) results show that a non-H-bonding carrier ligand can completely favor an HH1 conformer. Even more compelling are the results revealed in an X-ray structure of a duplex with a monofunctional Pt adduct, *cis*-Pt(NH_3)$_2$(pyridine)(oligo).[21,22] The pyridine ring of this adduct would be in severe steric clash with the XpG* phosphodiester group if the X·X′ bp did not reposition to create a bp step with an unusual positive slide and shift, as found with difunctional Pt adducts. In this very interesting adduct, the sugar pucker at both the X and G* residues is S. Thus, it is clear that while the underlying steric cause of the unusual bp step is similar in XG* and XG*G* adducts, the 5′-G* pucker in the cross-link apparently induces an N pucker in the X residue.

There seems little doubt, however, that for a monoadduct the *cis*-amine is normally not placed such as to create the steric clash. The Pt(diethylenetriamine)(oligo) duplexes have no distortions,[78,79] as is also true for Pt(NH_3)$_3$(oligo) duplexes.[79,80] Thus, as a component of our analysis, we believe that the cross-link structure (dictated by stronger energy terms arising from the demands of the macrocyclic ring, the need to form WC base pairs, etc.) positions the Pt moiety in such a way as to enhance the steric effect of the NH_3 in cisplatin adducts closest to the 5′-X residue. The pronounced steric effect of the pyridine ring in *cis*-Pt(NH_3)$_2$(pyridine) monoadducts induces the Lippard bp step without the aid of cross-link formation and with no involvement of H-bonding by the Pt moiety and the 5′-X residue. This interpretation raises the rather interesting hypothesis that the key to the anticancer activity of Pt drugs is this XG* bp step distortion (a distortion which escaped notice and definition for many years). Indeed, such a possibility has recently been independently suggested.[22]

Conclusions

We conclude that the movement of the 5′-X residue base to avoid steric clashes with the carrier ligand and to form a base pair, not the change from L to R canting, is the main cause of the weak carrier-ligand H-bonding and the relatively unusual features distinctive to the "Lippard bp step". Although compelling evidence and arguments are presented in this work that steric clashes are the main drivers for the unusual features of the Lippard bp step, the growing importance of this feature, combined with its unusual characteristics, dictates that additional studies be designed to elucidate this chemistry. In particular, we agree with a reviewer comment that the carrier ligand effects are important and need to be better understood. Toward this end, we are currently investigating the effects of both increasing and decreasing carrier ligand bulk relative to the bulk of the Bip ligands used in this study.

Acknowledgment. This work was supported by the University of Bari and EC (COST Action D39) (G.N.).

Supporting Information Available: Complete description of ^{1}H NMR signal assignments for G* residues of the HH1 R conformer of (*R*,*S*,*S*,*R*)-BipPt(oligo) adducts, shifts of the G H8 signals of the free oligos, regions of NOESY spectra of the various adducts, ^{1}H NMR spectra of various adducts as a function of temperature, ^{31}P NMR spectra for (*R*,*S*,*S*,*R*)-BipPt(oligo) adducts, comparison of structures having different torsion angles, and a stereoview of an (*R*,*S*,*S*,*R*)-BipPt(d-(TG*G*T)) structure. This material is available free of charge via the Internet at http://pubs.acs.org.

JA903787M

(75) Natile, G.; Marzilli, L. G. *Coord. Chem. Rev.* **2006**, *250*, 1315–1331.
(76) Carlone, M.; Marzilli, L. G.; Natile, G. *Eur. J. Inorg. Chem.* **2005**, 1264–1273.
(77) Carlone, M.; Marzilli, L. G.; Natile, G. *Inorg. Chem.* **2004**, *43*, 584–592.
(78) Macquet, J. P.; Butour, J. L. *Eur. J. Biochem.* **1978**, *83*, 375–385.
(79) Keck, M. V.; Lippard, S. J. *J. Am. Chem. Soc.* **1992**, *114*, 3386–3390.
(80) van Garderen, C. J.; Altona, C.; Reedijk, J. *Inorg. Chem.* **1990**, *29*, 1481–1487.